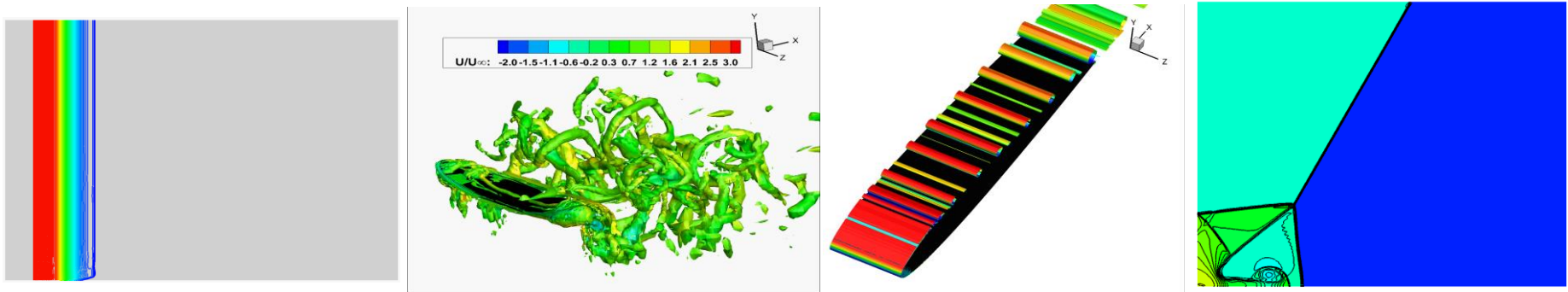


High-Order Numerical Simulation of Shock/Boundary Layer Interaction over Surface Roughness Using the FR/CPR-LLAV Method







Modeling Methods Session, TFAWS (NASA)

Meilin Yu, Assistant Professor
Department of Mechanical Engineering
University of Maryland, Baltimore County

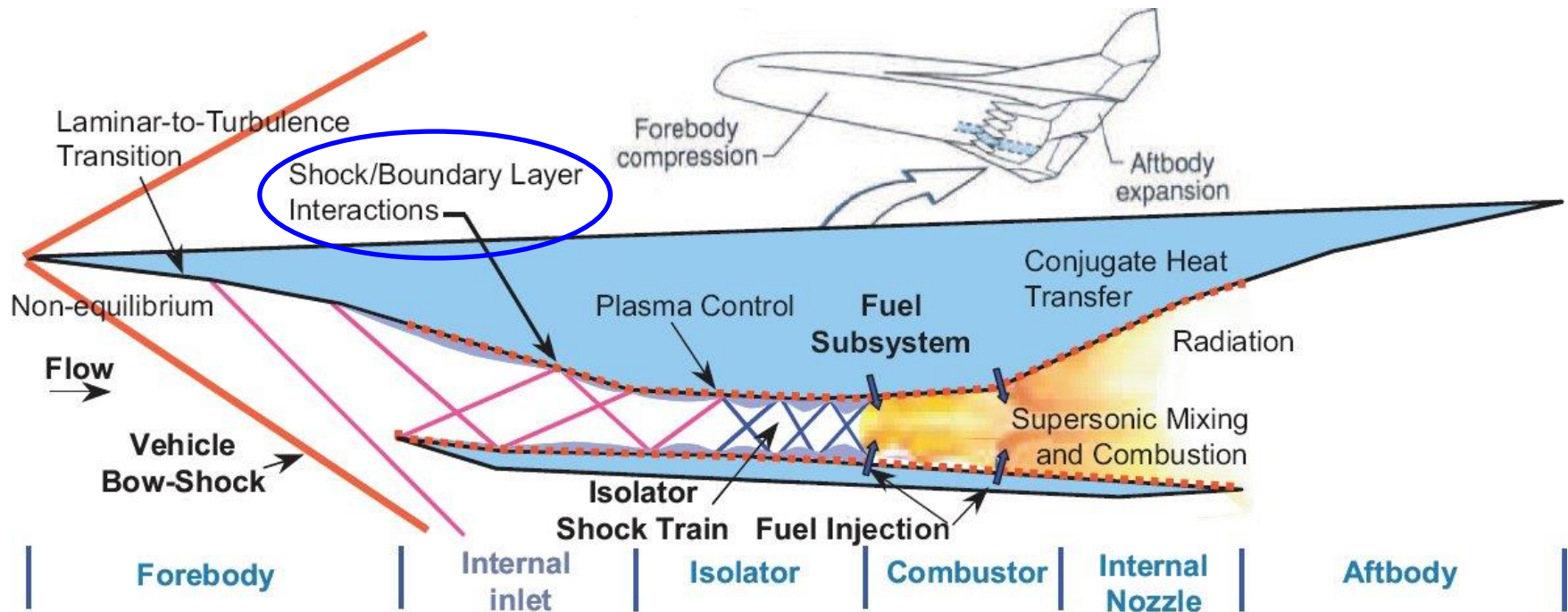
Contents

-  **Background**
-  **Numerical Methods & Verification**
-  **Shock/Boundary Layer Interaction (SBLI)**
 - **SBLI over smooth walls**
 - **SBLI over surface roughness**
-  **Conclusions & Future Work**

Contents

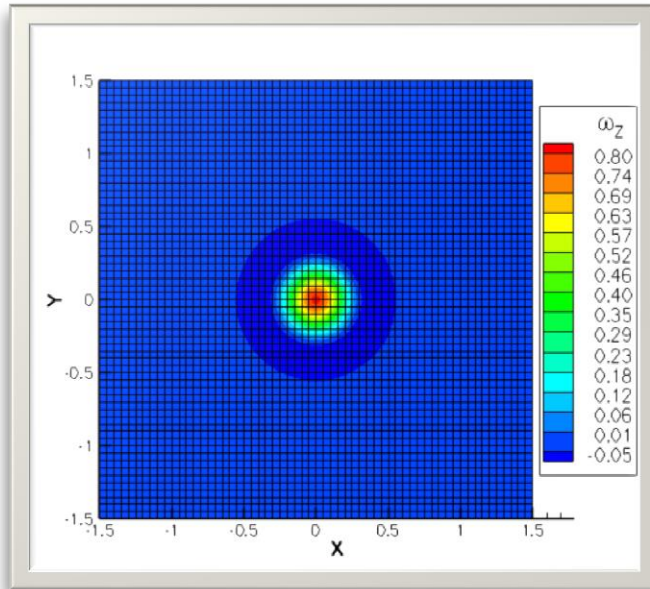
-  **Background**
-  Numerical Methods & Verification
-  Shock/Boundary Layer Interaction (SBLI)
 - SBLI over smooth walls
 - SBLI over surface roughness
-  Conclusions & Future Work

Background

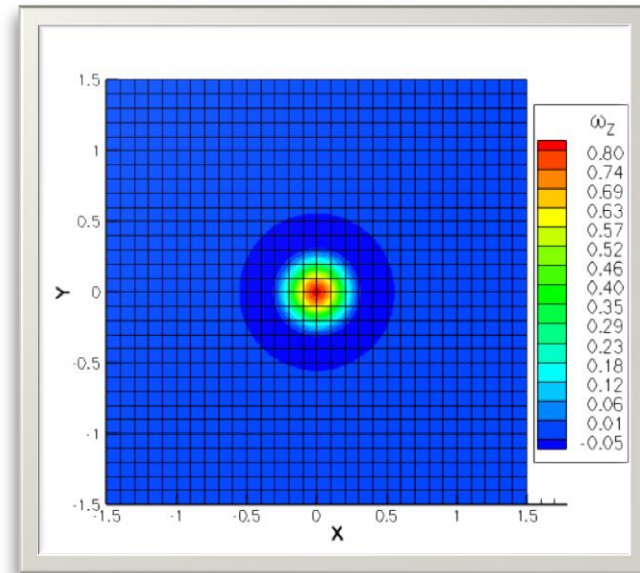


Schematics of fluid flow and heat transfer in a scramjet engine
(Source: FPCE group, Stanford University)

Why High-Order CFD Methods?



2nd order



4th order

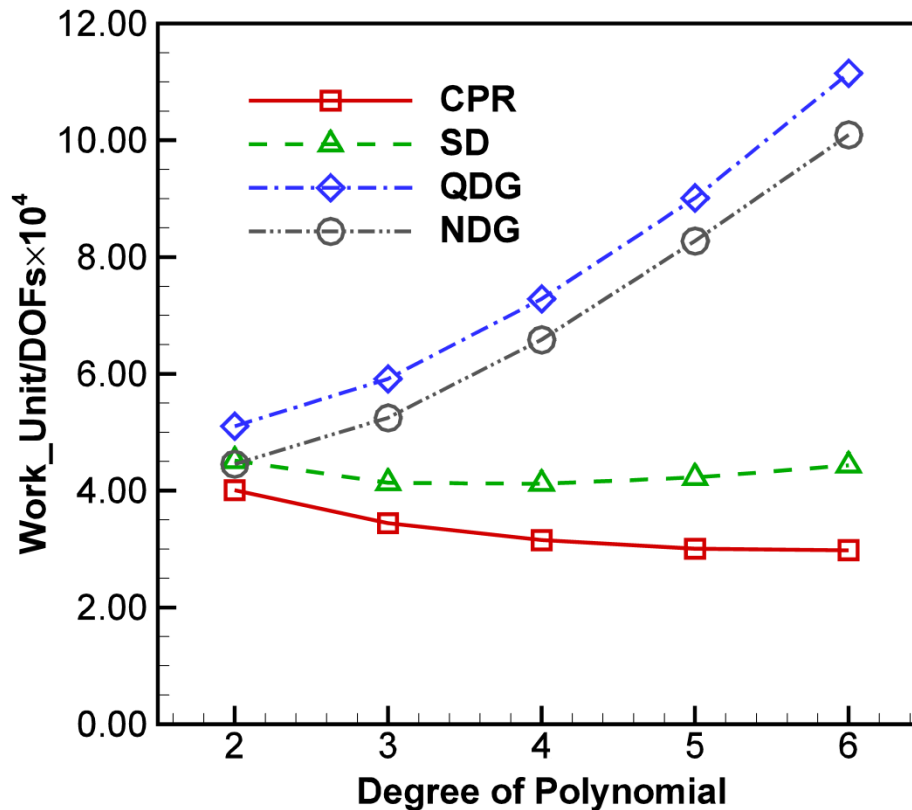
DOFs* for the 2nd order scheme: $(60 \times 60) \times 4 = 14400$

DOFs for the 4th order scheme: $(30 \times 30) \times 16 = 14400$

Euler vortex propagation

*: DOFs is short for degrees of freedom

Computational Cost of High-Order Methods



Computational cost per degree of freedom vs. polynomial order
Euler vortex propagation, linear elements

Objectives

- **Develop robust localized Laplacian artificial viscosity (LLAV) shock capturing procedures for the high-order flux reconstruction/correction procedure via reconstruction (FR/CPR) method**
- **Explore flow physics of complex shock-boundary layer interaction over surface roughness with the high-order FR/CPR-LLAV method**

Contents

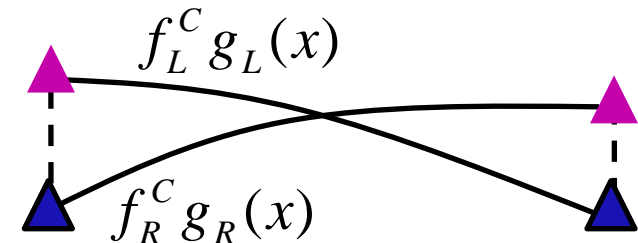
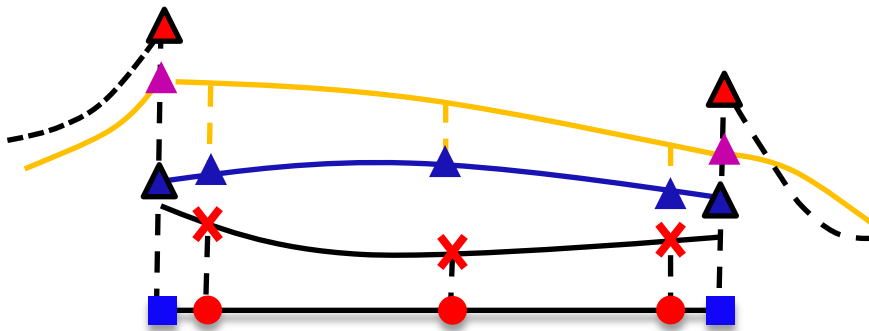
- Background
- **Numerical Methods & Verification**
- Shock/Boundary Layer Interaction (SBLI)
 - SBLI over smooth walls
 - SBLI over surface roughness
- Conclusions & Future Work

Flux Reconstruction/Correction Procedure via Reconstruction (FR/CPR)

➤ First developed by H. T. Huynh (2007)

$$\frac{\partial Q}{\partial t} + \frac{\partial f}{\partial x} = 0 \rightarrow \frac{\partial Q_h}{\partial t} + \frac{\partial f_h^I}{\partial x} = 0, \quad Q_h \in P^k(\Omega), \quad f_h^I \in P^{k+1}(\Omega)$$

$$\frac{\partial f_h^I}{\partial x} = \frac{\partial (f_h^D + f_h^C)}{\partial x}, \quad f_h^D \in P^k(\Omega), \quad f_h^C \in P^{k+1}(\Omega)$$



$$f_h^C(x) = f_L^C g_L(x) + f_R^C g_R(x)$$

- Very efficient high-order algorithm
- Generalization of discontinuous Galerkin and spectral difference/volume
- Compact, suitable for parallel computation

Localized Laplacian Artificial Viscosity

$$\frac{\partial Q}{\partial t} + \nabla \cdot \mathbf{F}^{inv}(Q) = \nabla \cdot \mathbf{F}^{av}(Q, \nabla Q)$$

Laplacian: $\mathbf{F}^{av}(Q, \nabla Q) = \varepsilon \nabla Q$

For each element e :

$$\varepsilon_e = \begin{cases} 0 & \text{if } S_e < S_0 - \kappa \\ \frac{\varepsilon_0}{2} \left(1 + \sin \frac{\pi(S_e - S_0)}{2\kappa} \right) & \text{if } S_0 - \kappa \leq S_e \leq S_0 + \kappa \\ \varepsilon_0 & \text{if } S_e > S_0 + \kappa. \end{cases}$$

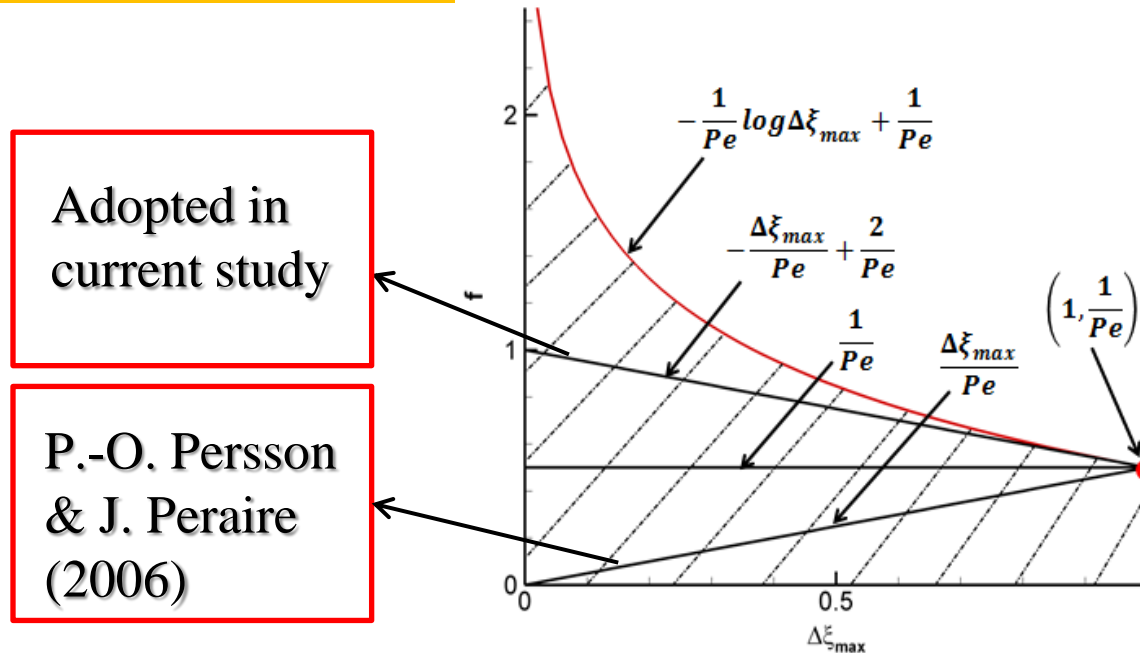
Parameters in ε_e :

$\varepsilon_0 = f(\Delta \xi_{max}, Pe) \cdot h \cdot |\lambda|_{max}$, based on the definition of the *Péclet* number Pe for a diffusion process:

Resolution-based smoothness indicator:

$$S_e = \log_{10} \frac{\langle Q - Q^{proj}, Q - Q^{proj} \rangle_e}{\langle Q, Q \rangle_e},$$

Localized Laplacian Artificial Viscosity (Cont.)

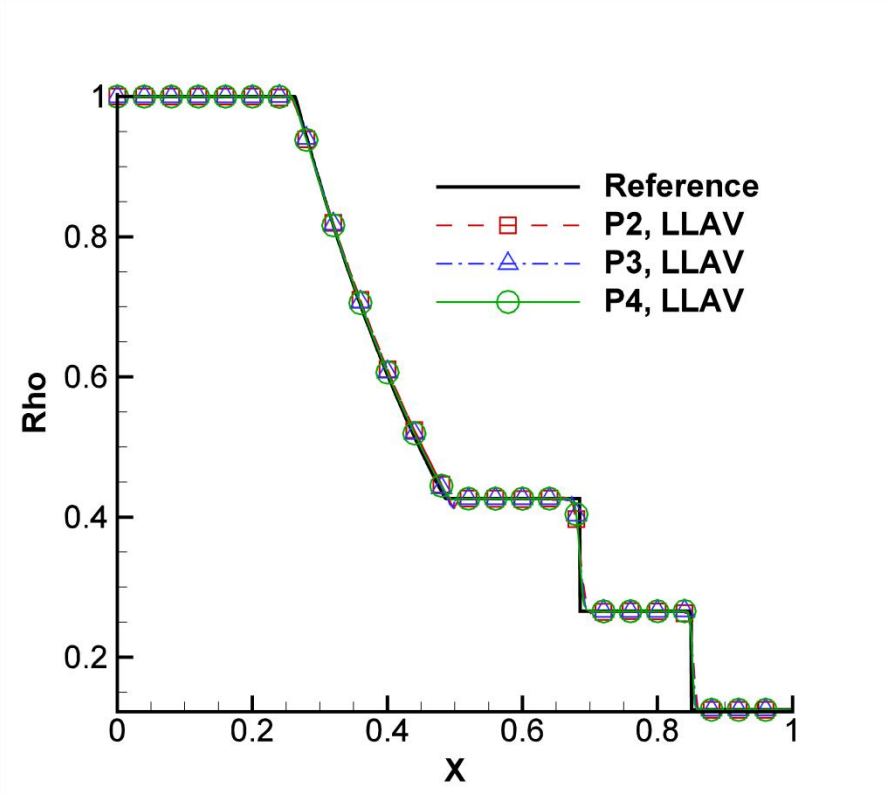


Modeling criteria:

- The artificial viscosity ε_0 is non-negative;
- When the resolution of the numerical scheme is infinite, the artificial viscosity $\varepsilon_0 \rightarrow 0$;
- The modeling is compatible with the classic results from the 2nd order accurate (or equivalently P^1 reconstruction) methods.

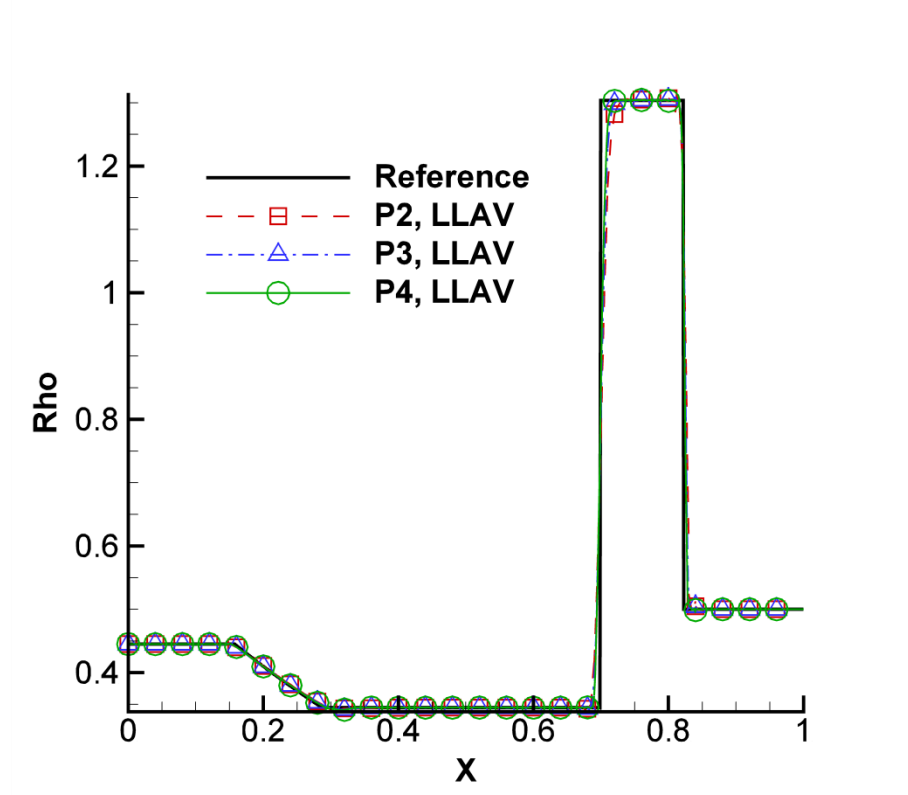
1D Shock Tube Problem

Sod Problem



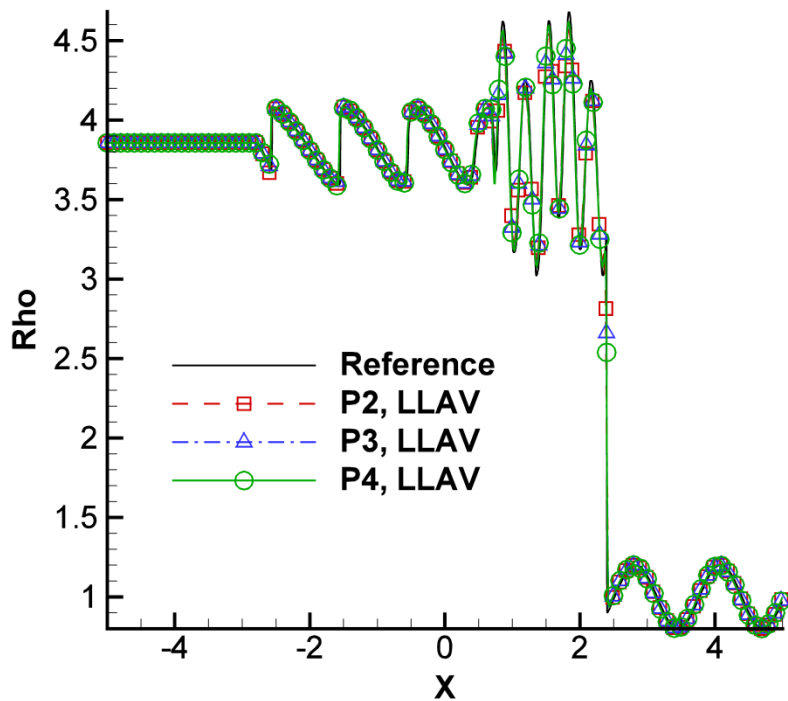
Density distribution at $t = 0.2s$

Harten-Lax Problem

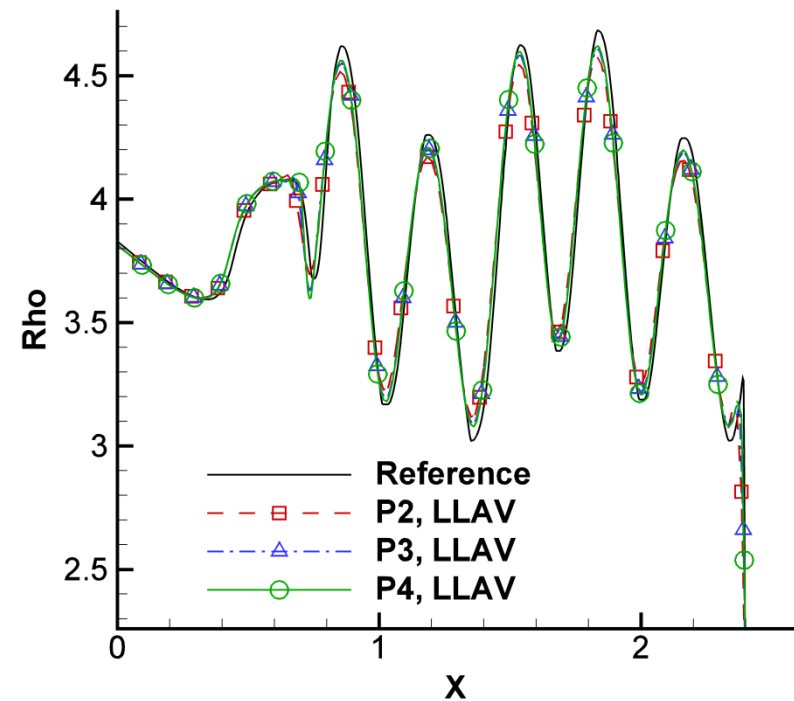


Density distribution at $t = 0.13s$

Shu-Osher Problem



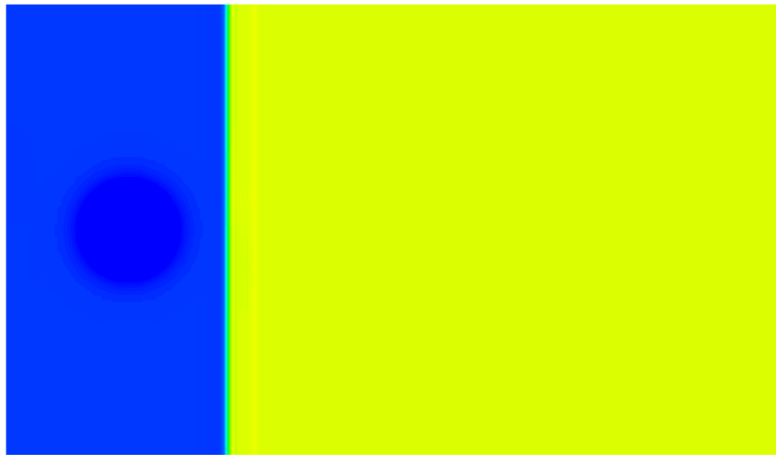
Overview



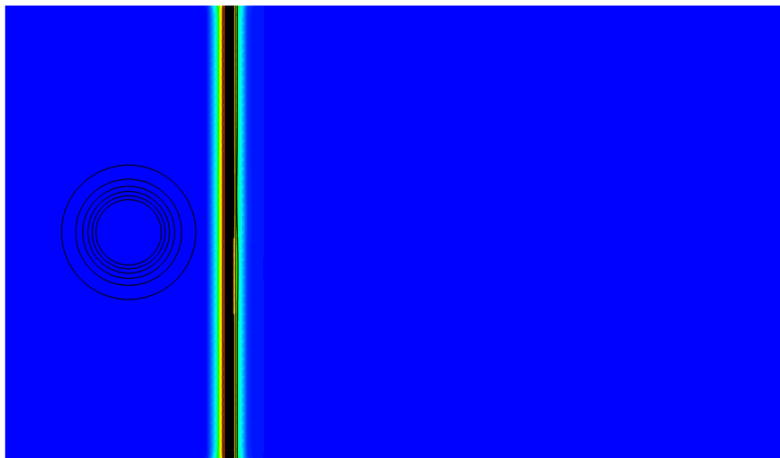
Close-up view

Density distribution at $t = 1.8s$

Shock-Isentropic Vortex Interaction



Pressure



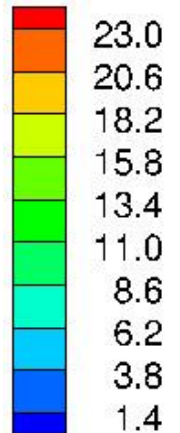
Artificial viscosity

Free stream $Ma = 1.1$,
 P^3 reconstruction (4th order),
Computational domain:
 $[0,2] \times [0,1]$,
100 \times 50 elements.

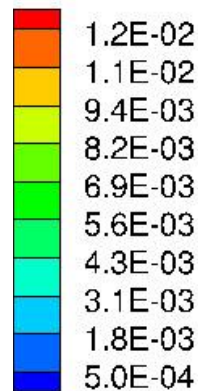
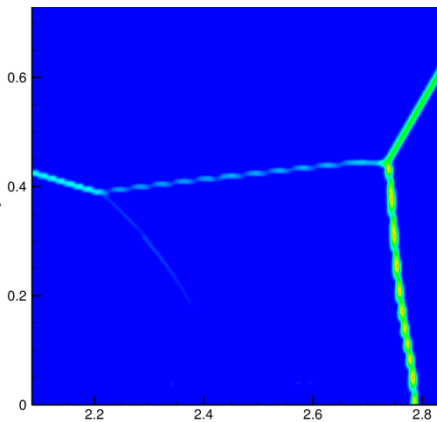
An isentropic vortex is
superposed to the supersonic
flow.

Double Mach Reflection

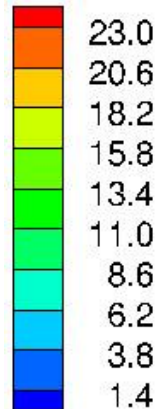
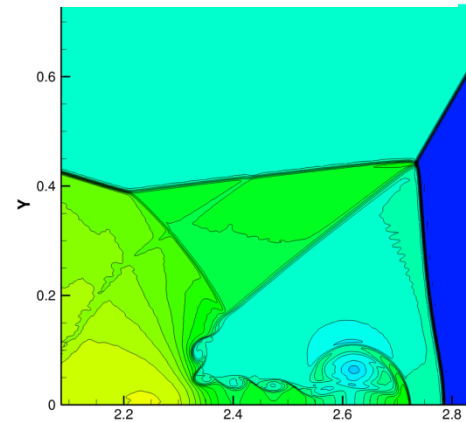
Density



Artificial
viscosity at
 $t=0.2s$



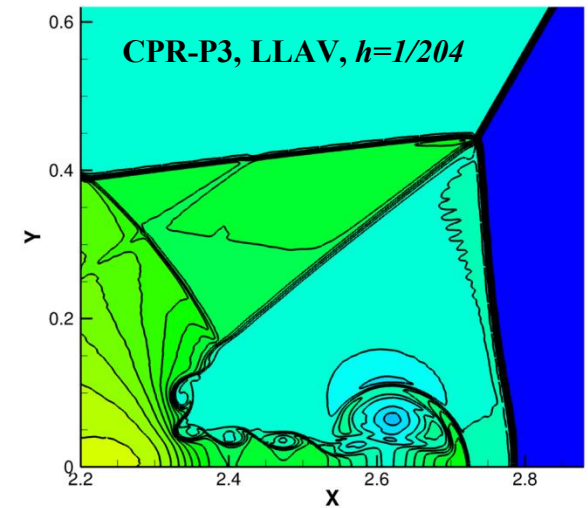
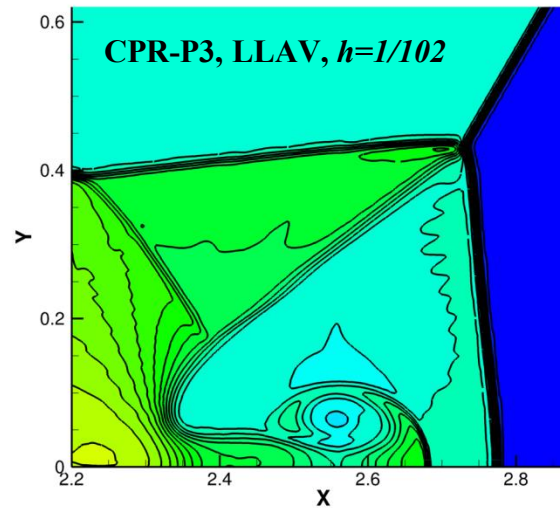
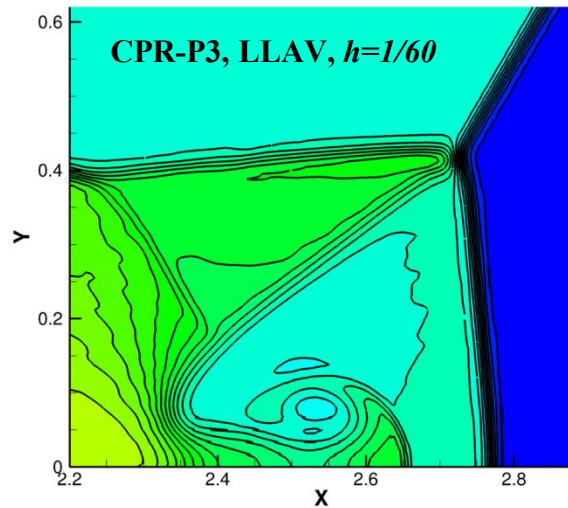
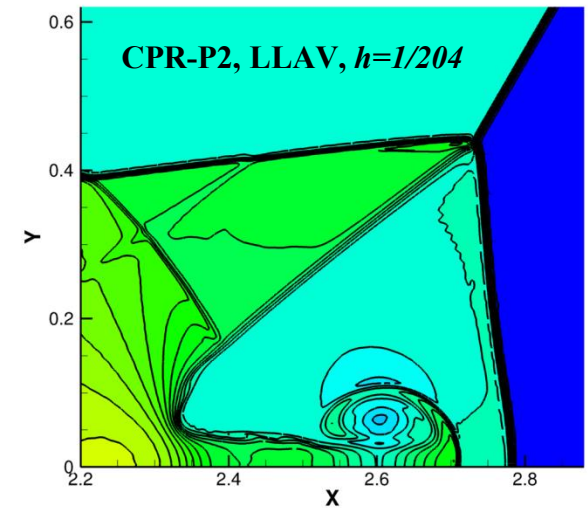
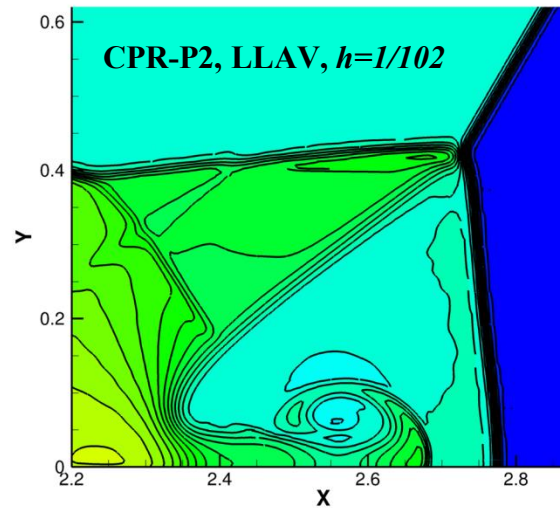
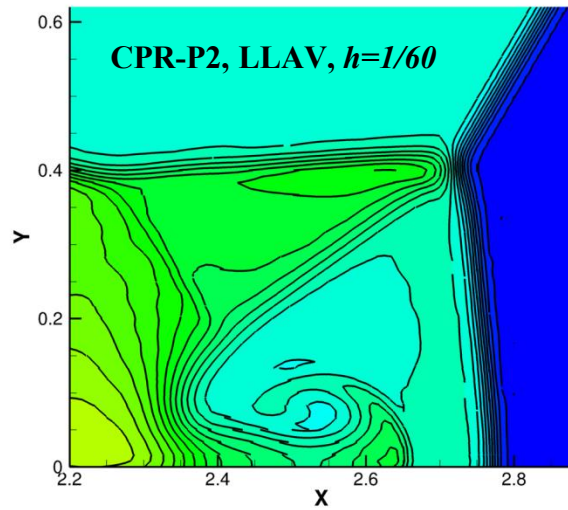
Density at
 $t=0.2s$



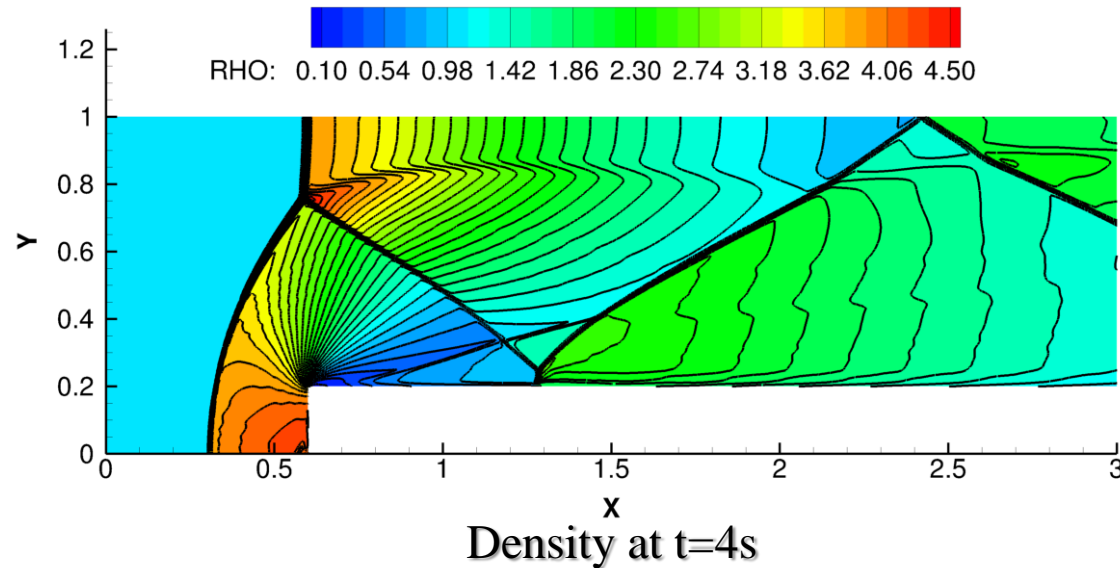
$Ma = 10$, P^3 reconstruction (4th order), $t \in [0, 0.2s]$

Computational domain $[0, 4] \times [0, 1]$, 816×204 elements

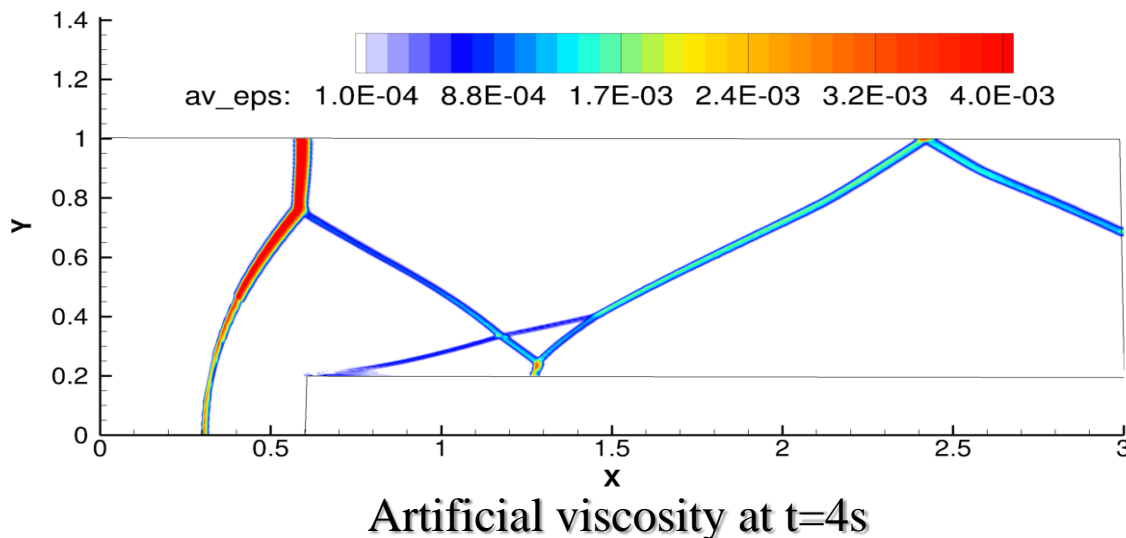
Double Mach Reflection (Cont.)



Ma 3 Wind Tunnel with a Forward Facing Step



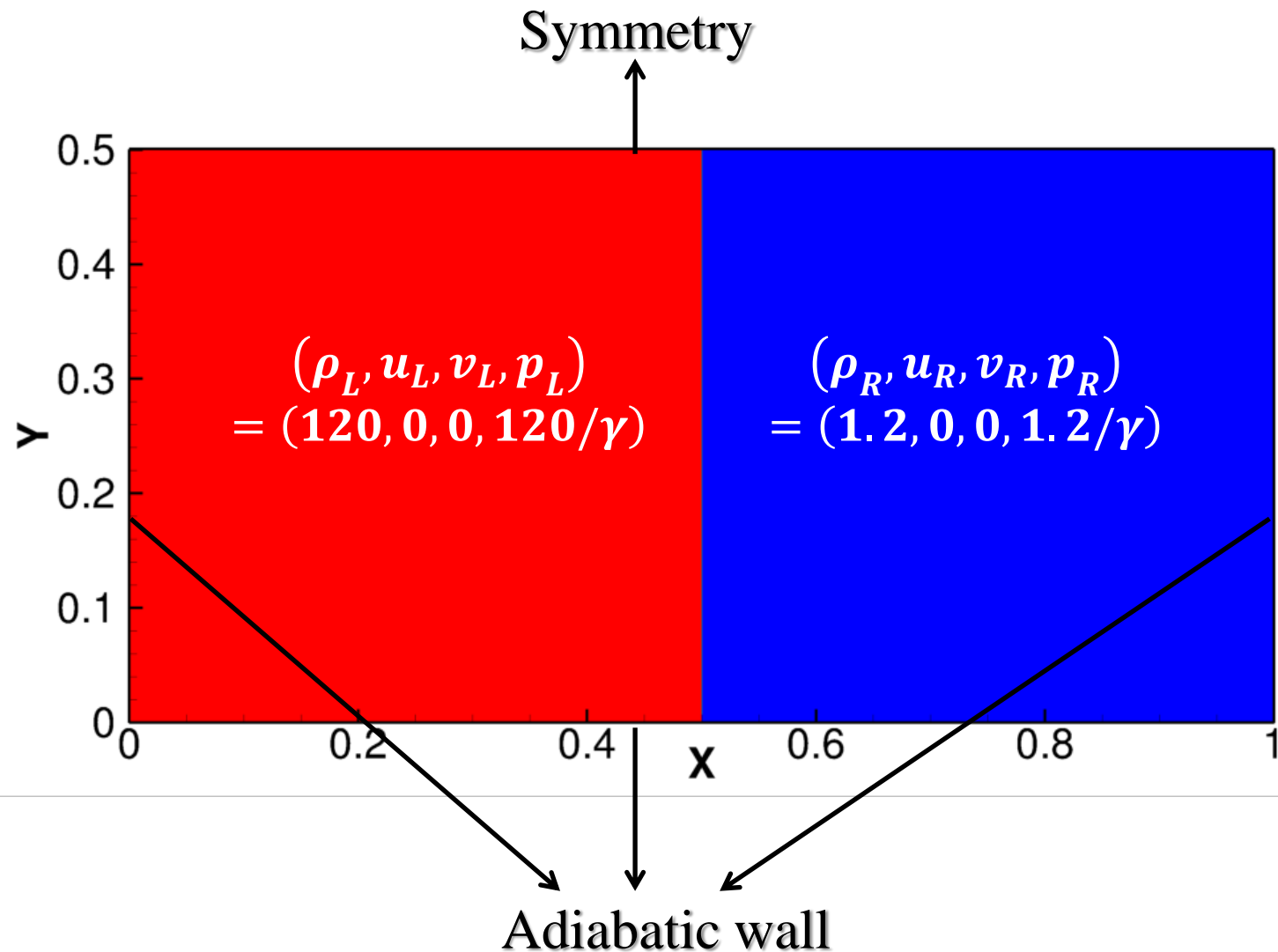
Free stream $Ma = 3$,
 P^2 reconstruction (3rd order),
 Grid size: 1/80, with
 clustered elements of
 size 1/320 near the
 sharp corner.



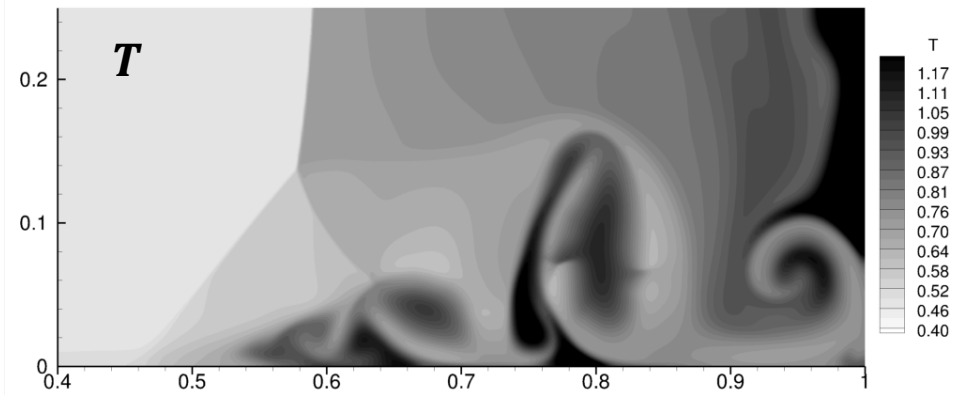
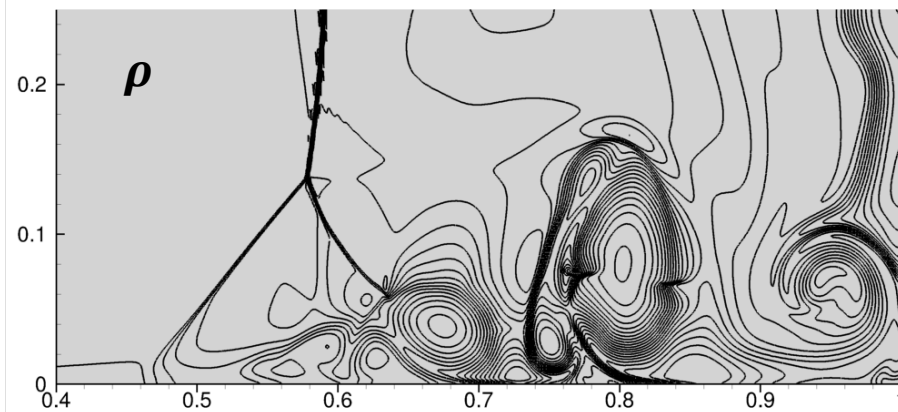
Contents

- ✚ Background
- ✚ Numerical Methods & Verification
- ✚ **Shock/Boundary Layer Interaction (SBLI)**
 - **SBLI over smooth walls**
 - SBLI over surface roughness
- ✚ Conclusions & Future Work

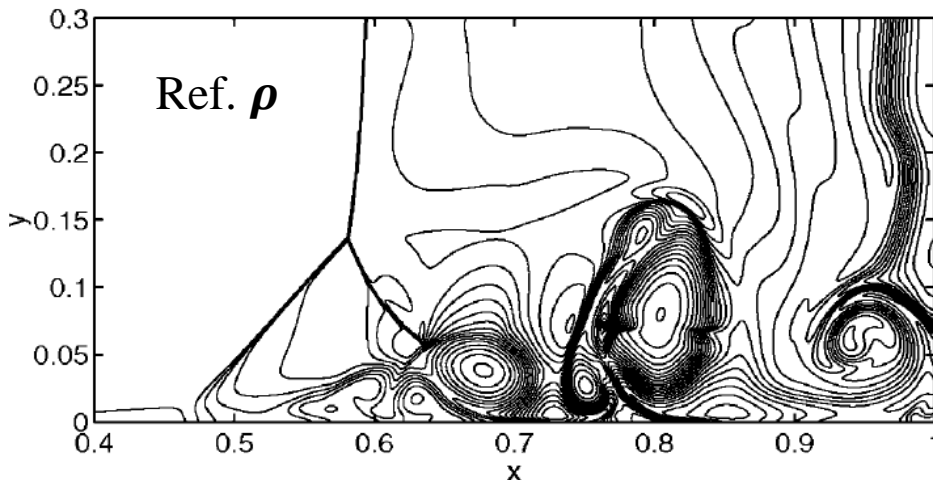
Initial & Boundary Conditions



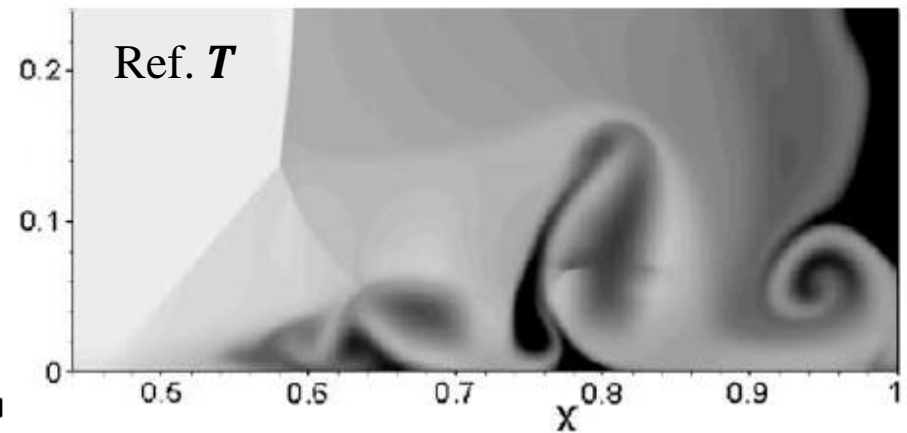
SBLI over Smooth Walls at $Re=200$



P^2 reconstruction on a 500×250 mesh (1.125×10^6 DOFs)

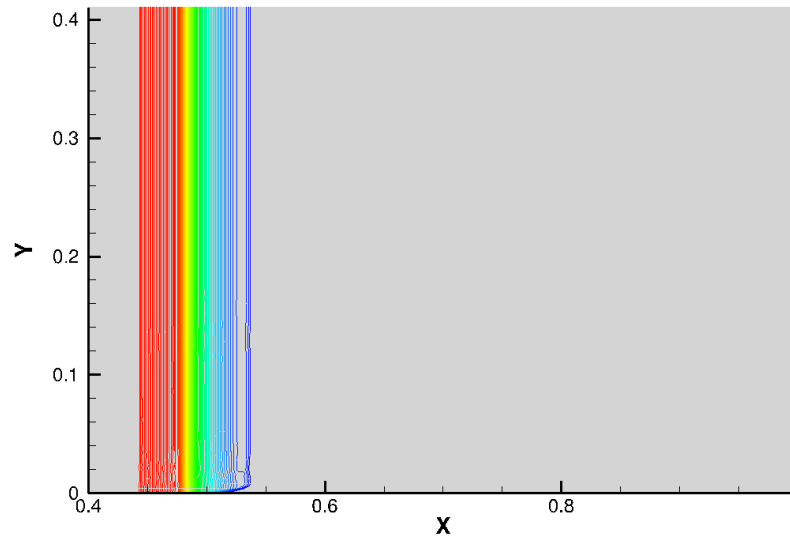


2nd order MUSCL scheme on a 3000×1500 mesh (4.5×10^6 DOFs) (Sjogreen & Yee, 2003)

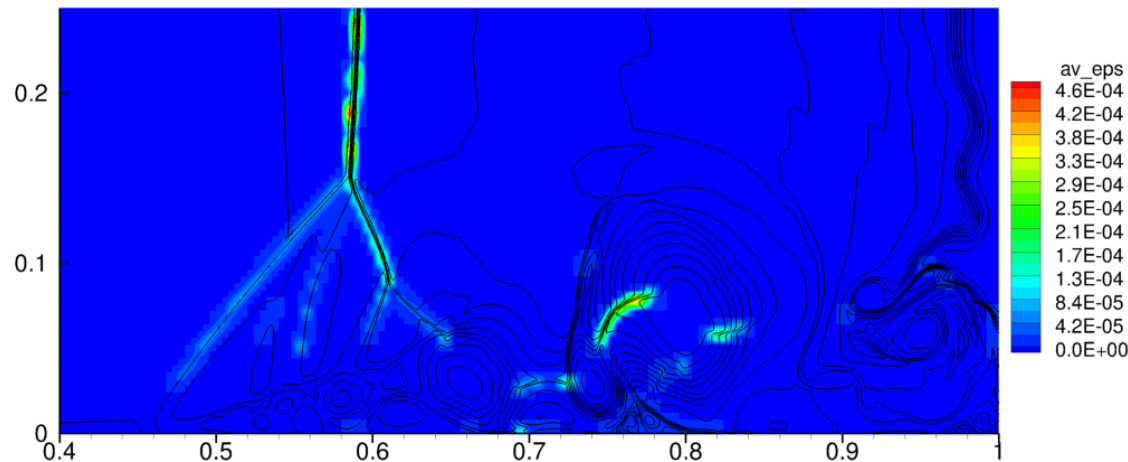


7th order FD scheme on a 1000×500 mesh (0.5×10^6 DOFs) (Daru & Tenaud, 2009)

SBLI over Smooth Walls at $Re=1,000$

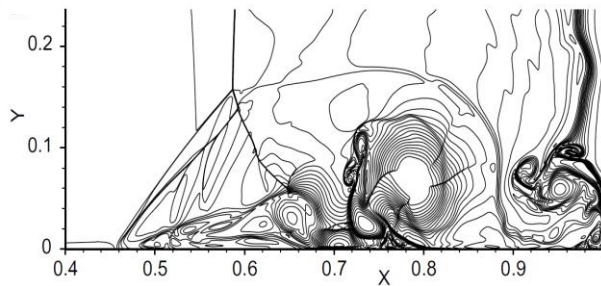
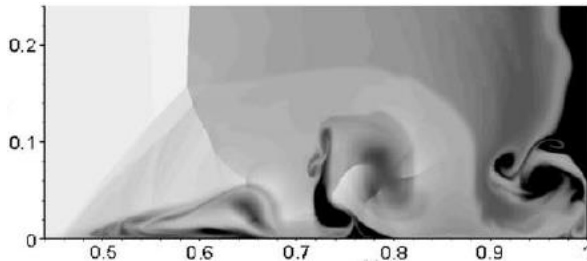


Density field

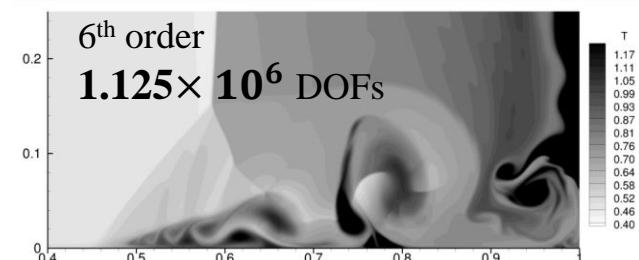
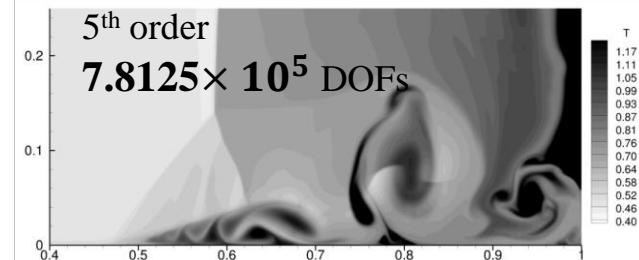
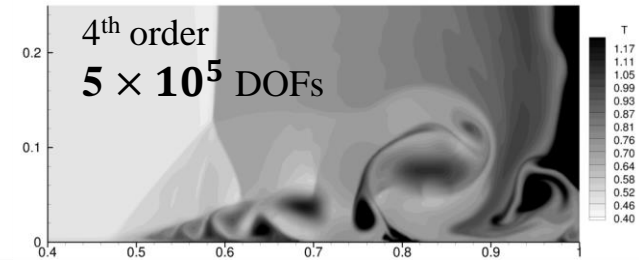
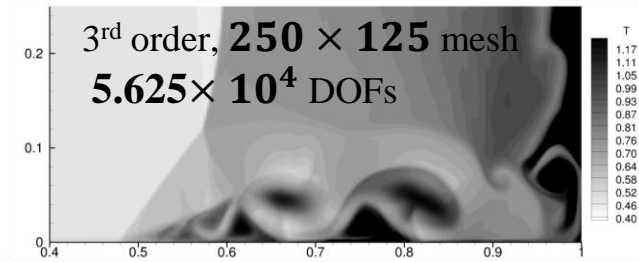
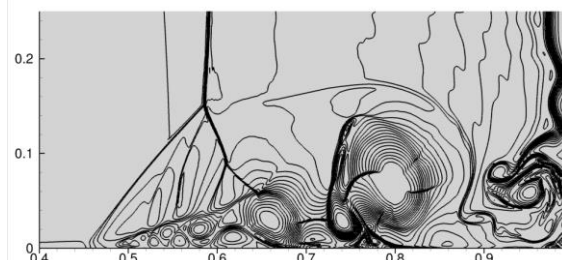
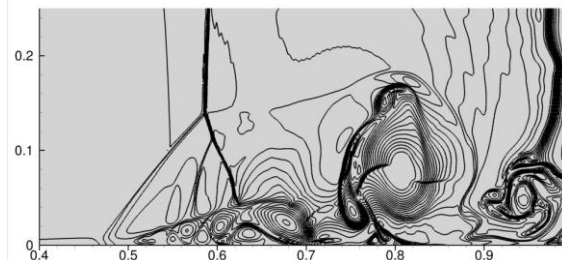
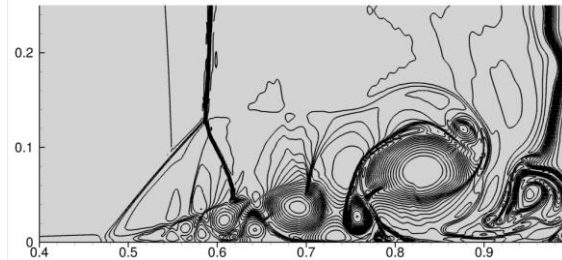
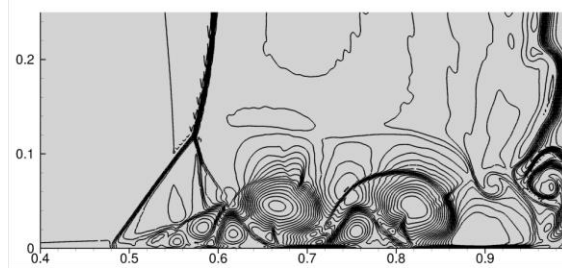


Distribution of
LLAV

SBLI over Smooth Walls at $Re=1,000$ (Cont.)



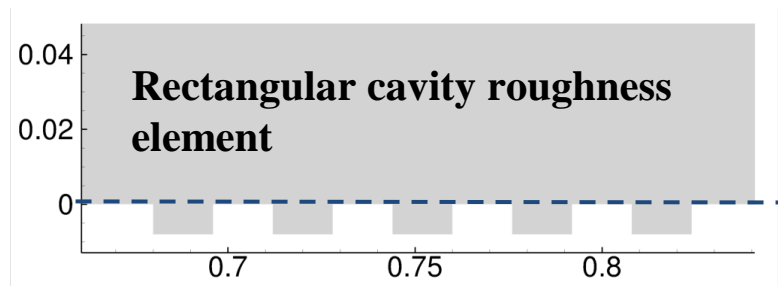
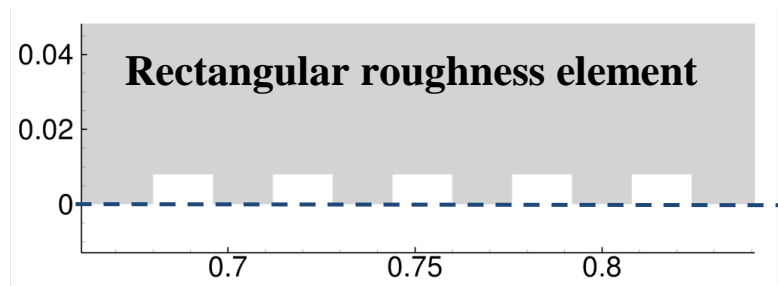
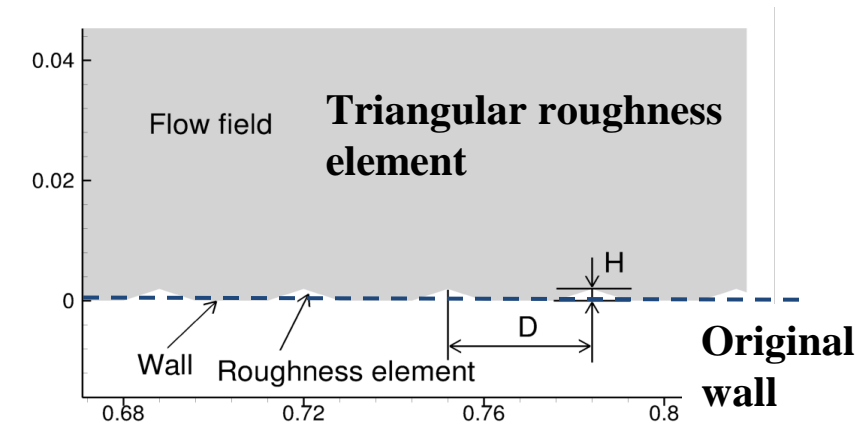
7th order FD scheme on a
 4000×2000 mesh
 $(8 \times 10^6 \text{ DOFs})$
 (Daru & Tenaud, 2009)



Contents

- ✚ Background
- ✚ Numerical Methods & Verification
- ✚ **Shock/Boundary Layer Interaction (SBLI)**
 - SBLI over smooth walls
 - **SBLI over surface roughness**
- ✚ Conclusions & Future Work

Wall Roughness Set-Up

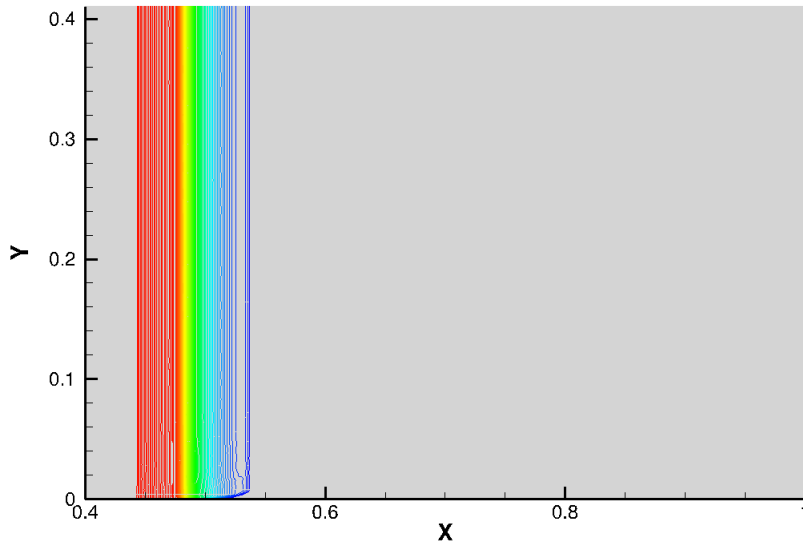


H/D	Triangular Element	Rectangular Element	Rectangular Cavity Element
1/32	Tri_H1	-	-
1/16	Tri_H2	-	-
1/8	Tri_H3	-	-
1/4	Tri_H4	Rec_H4	Rec_Cav_H4
1/2	-	-	Rec_Cav_H5

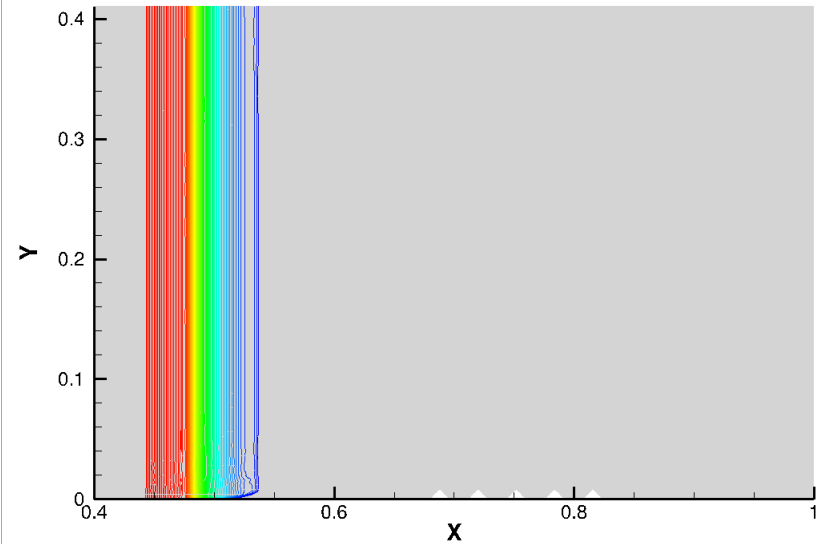
Cases summary

For all cases, the Reynolds number is $Re = 1,000$

SBLI over Triangular Surface Elements



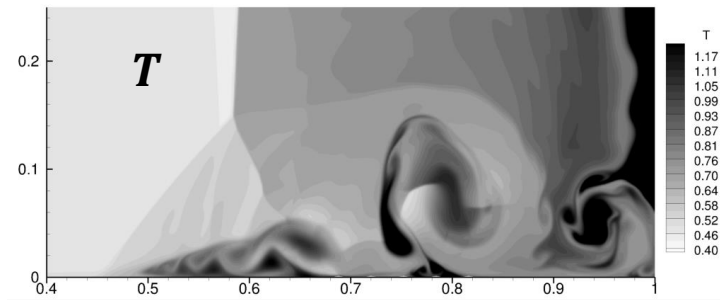
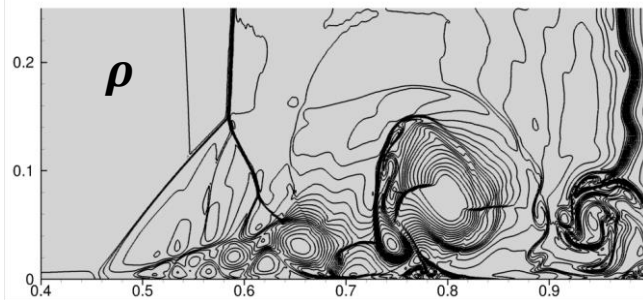
Tri_H1



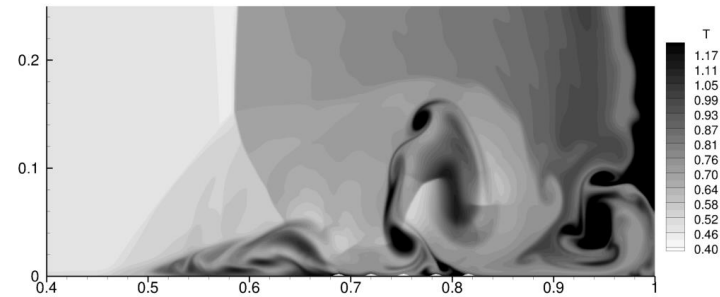
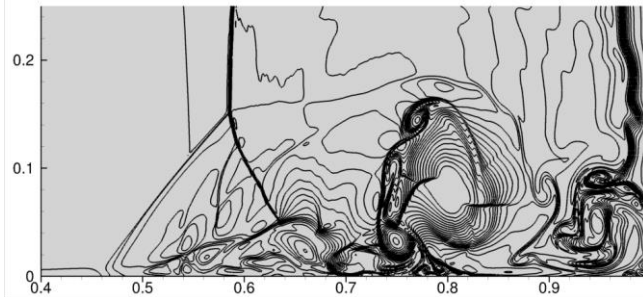
Tri_H4

Density fields

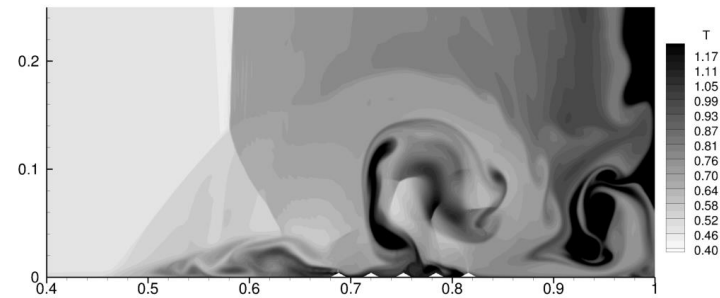
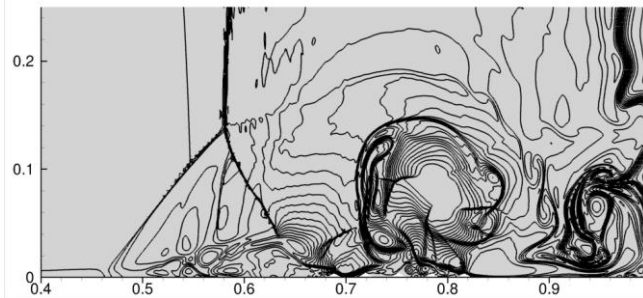
Flow Fields Comparison of Different H/D



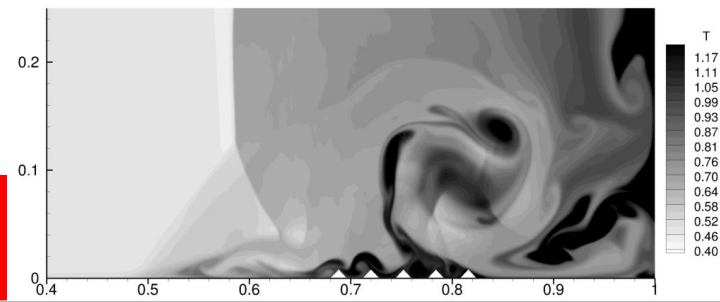
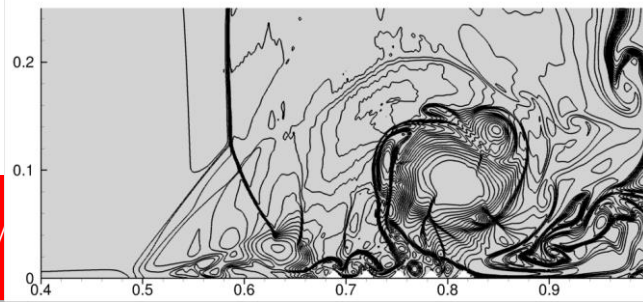
$$\frac{H}{D} = \frac{1}{32}$$



$$\frac{H}{D} = \frac{1}{16}$$

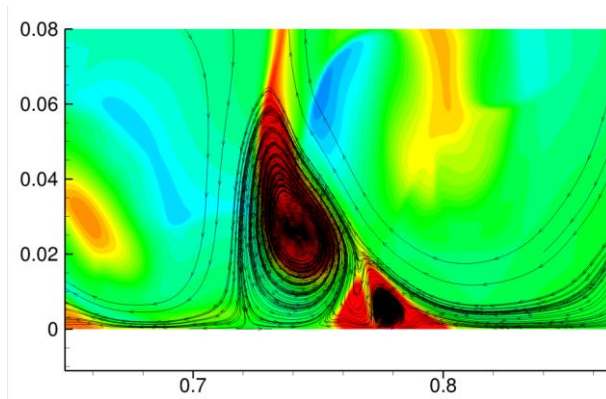


$$\frac{H}{D} = \frac{1}{8}$$

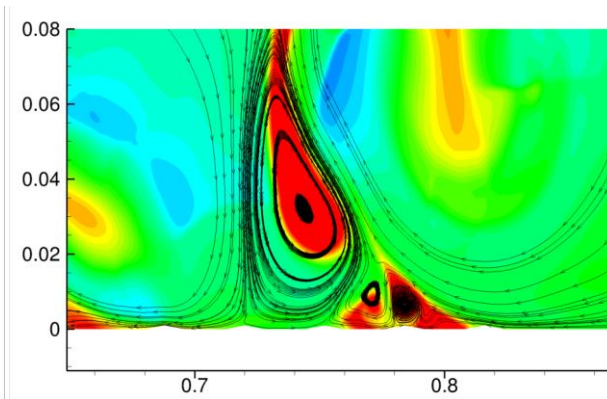


$$\frac{H}{D} = \frac{1}{4}$$

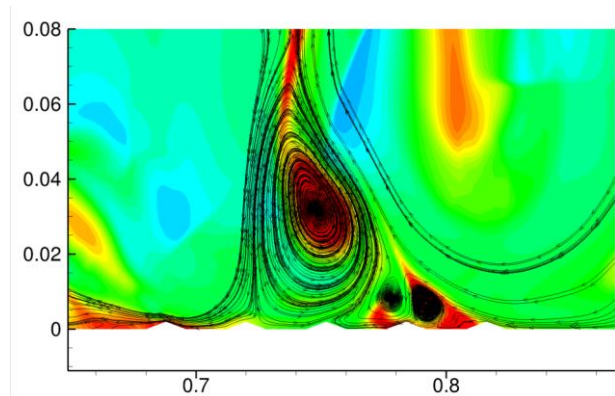
Streamlines & Temperature near Roughness



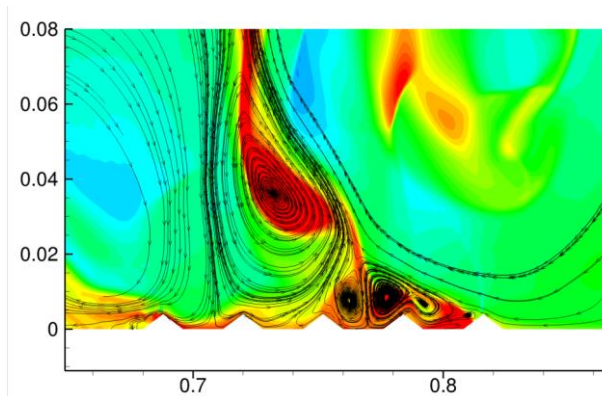
Smooth



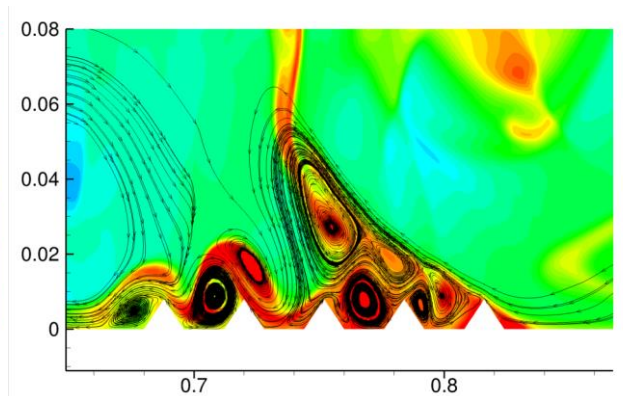
$H/D = 1/32$



$H/D = 1/16$

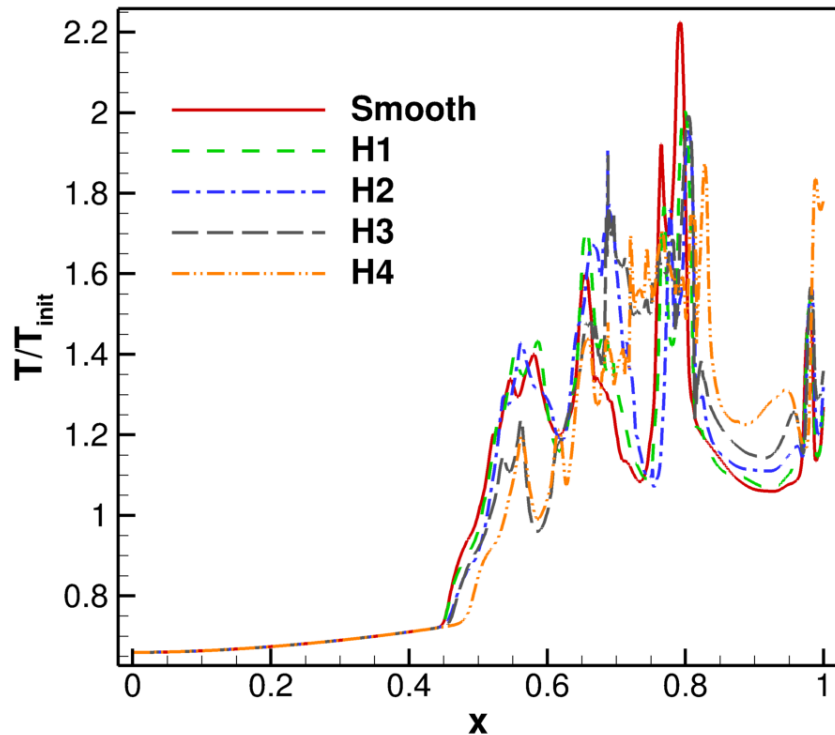


$H/D = 1/8$

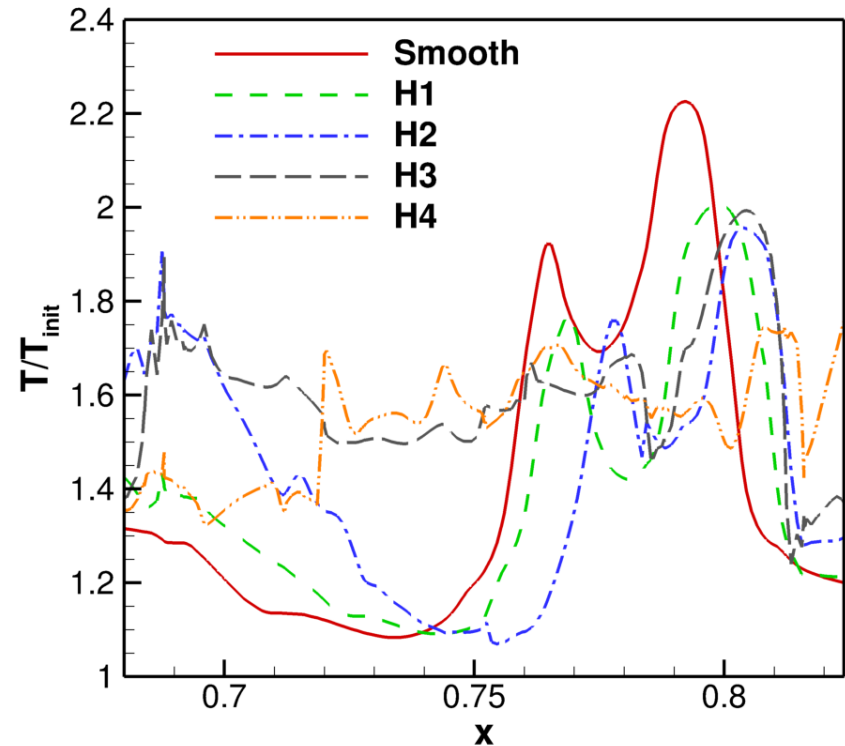


$H/D = 1/4$

Wall Temperature Comparison of Different H/D

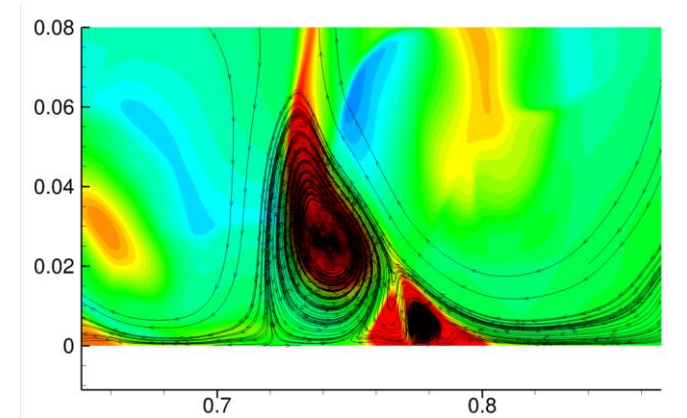
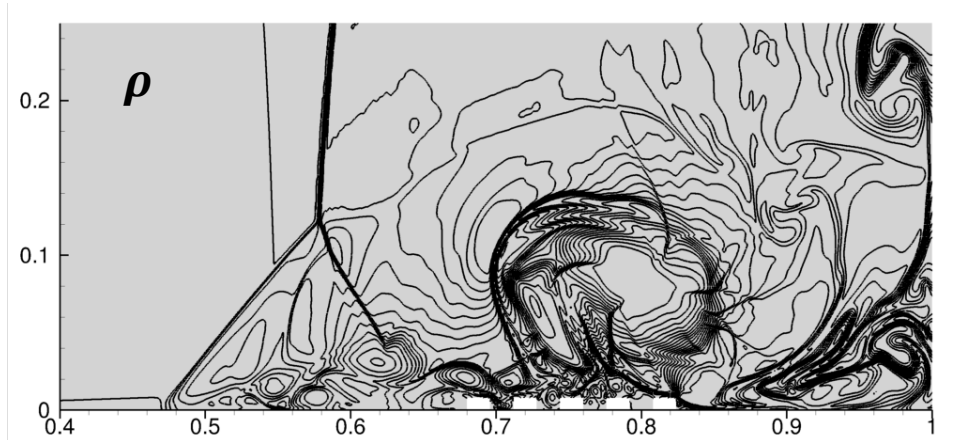


Overview of wall temperature

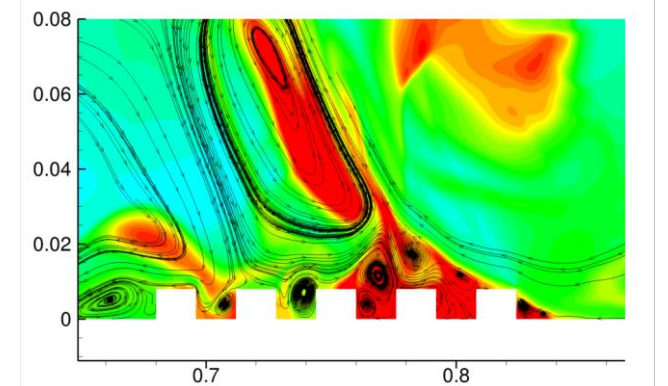
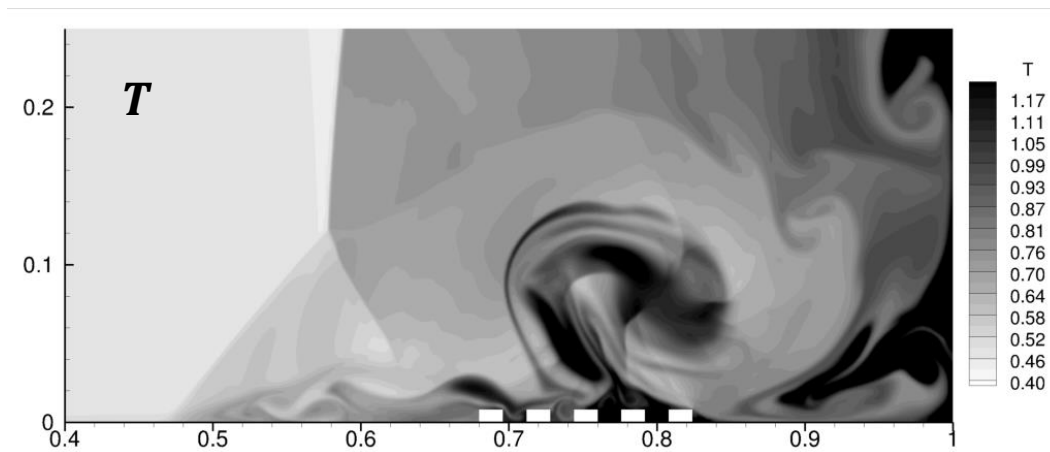


Close-up view of wall temperature

Flow Fields over Rectangular Roughness

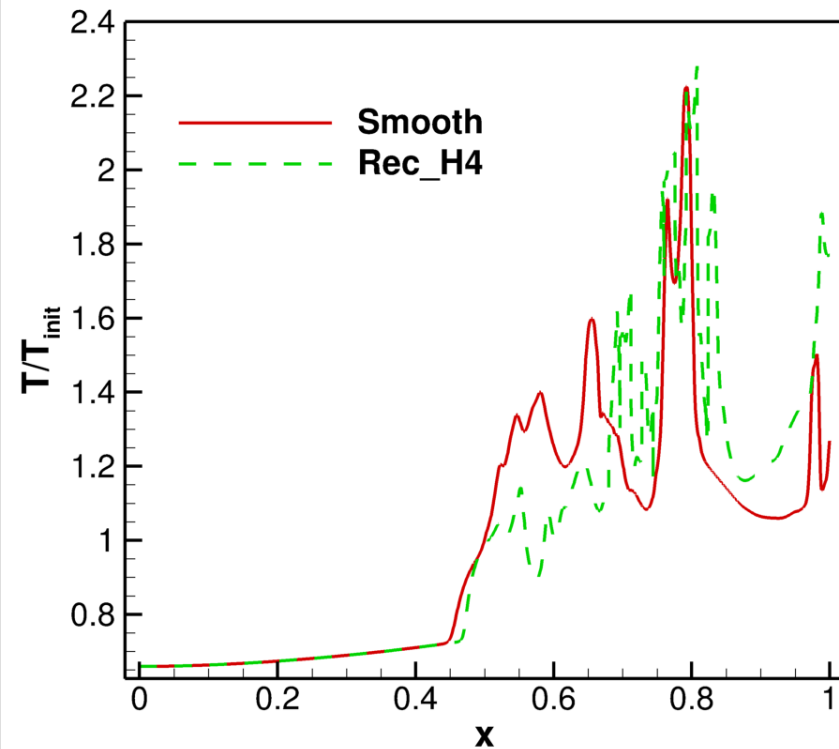


Smooth

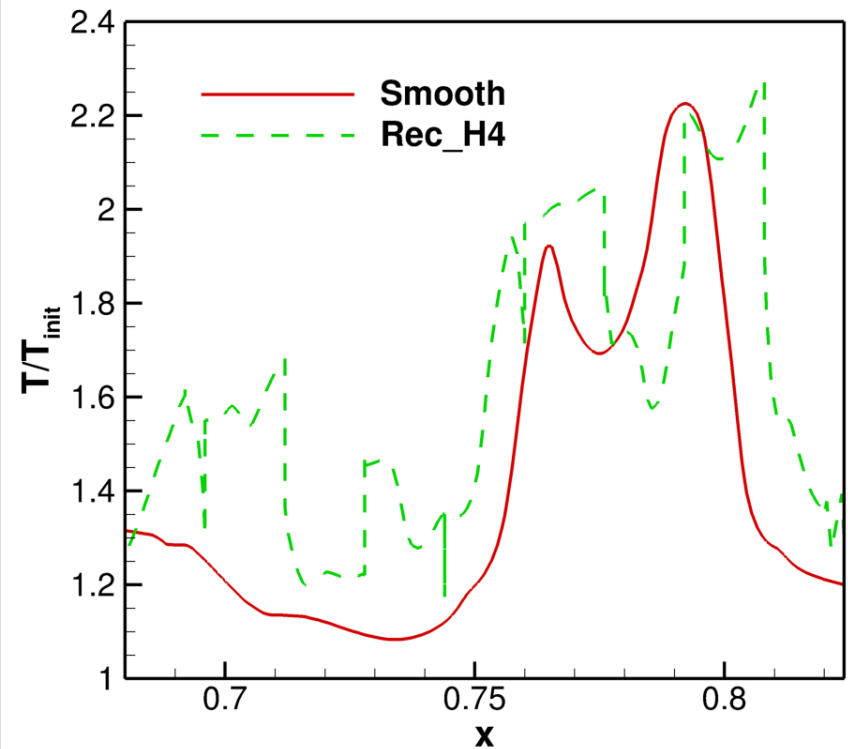


$H/D = 1/4$

Wall Temperature Comparison of Different H/D



Overview of wall temperature

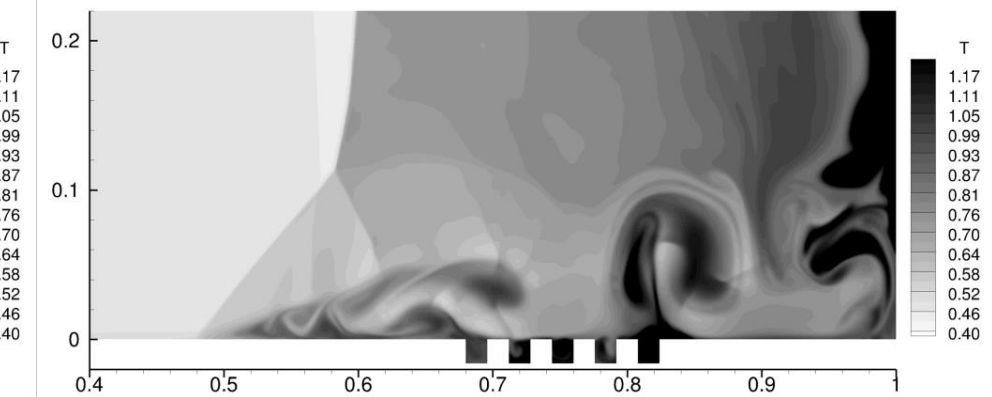
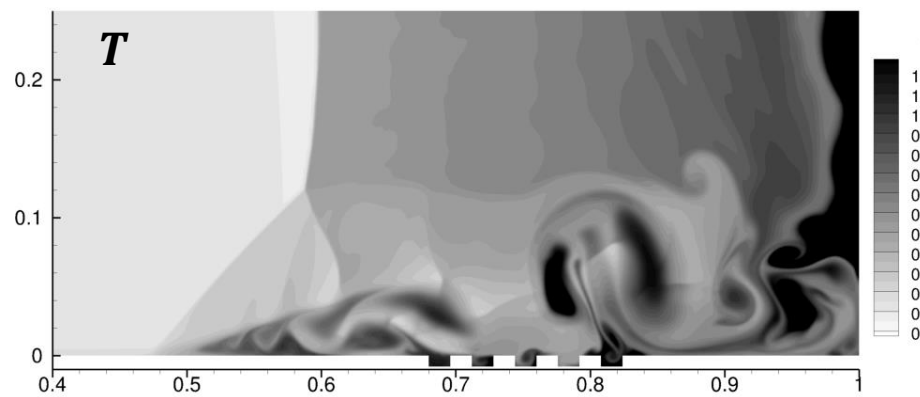
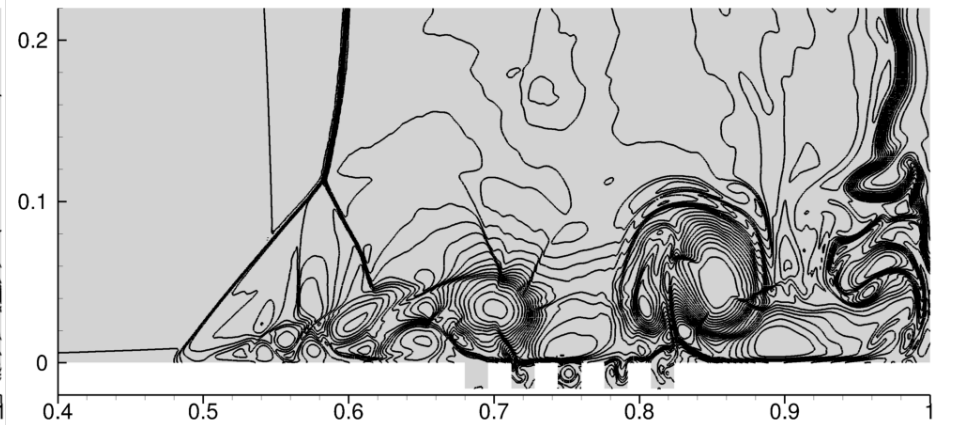
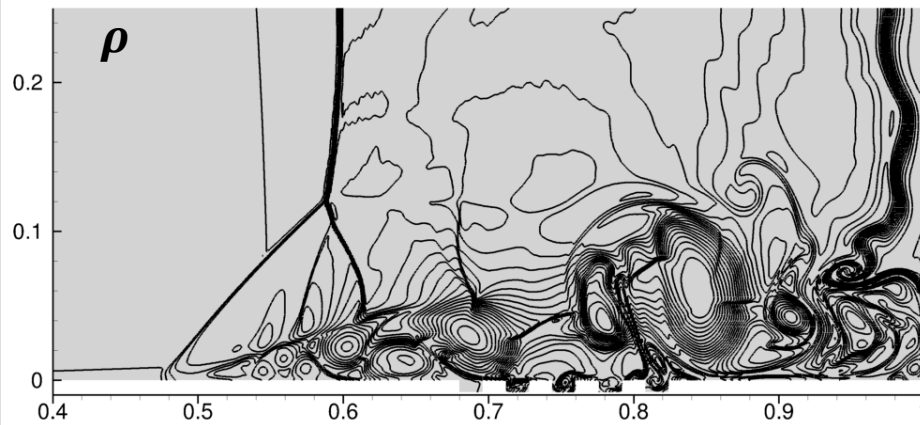


Close-up view of wall temperature

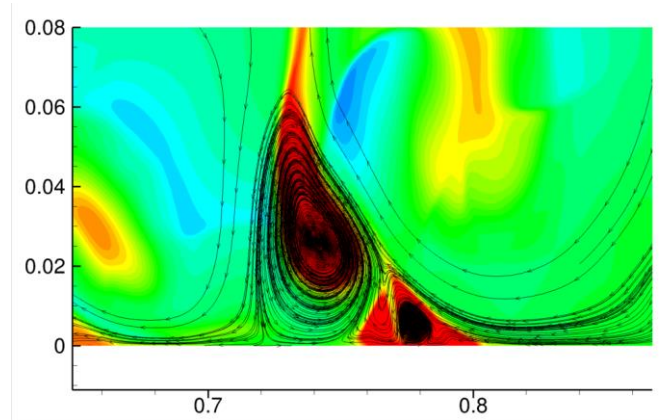
Flow Fields over Rectangular Cavity Roughness

$H/D = 1/4$

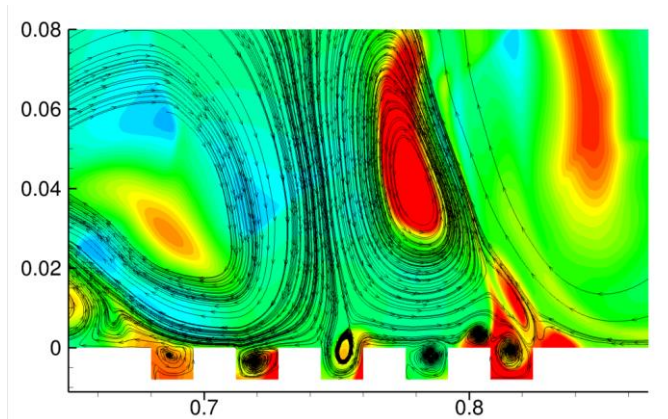
$H/D = 1/2$



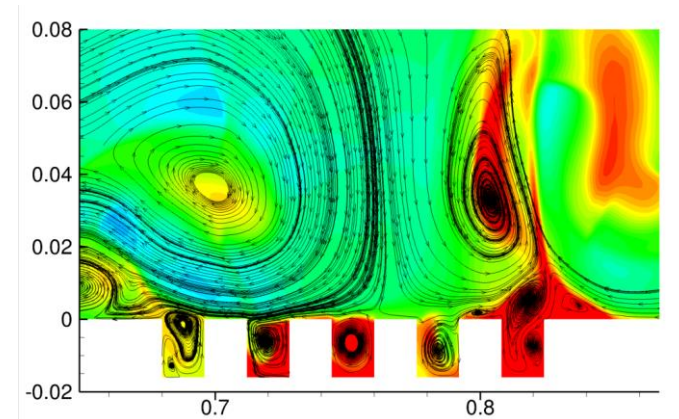
Streamlines & Temperature near Roughness



Smooth

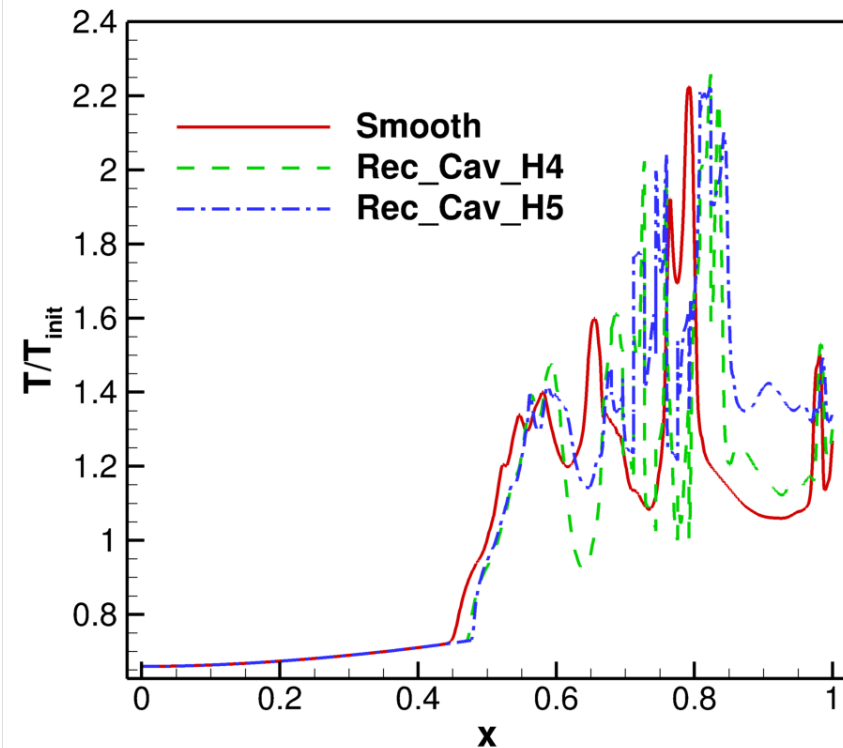


$H/D = 1/4$

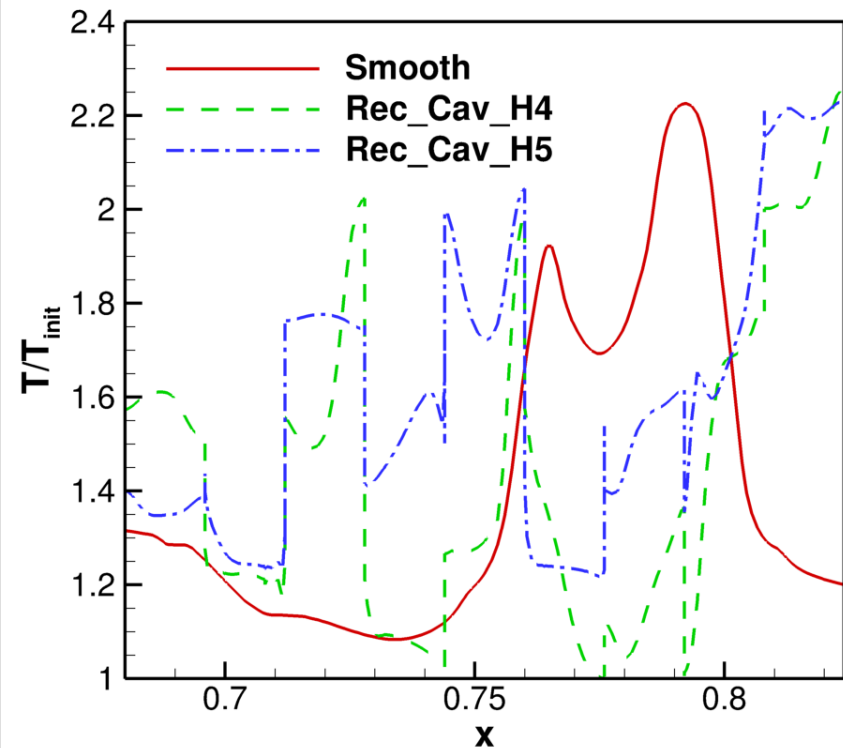


$H/D = 1/2$

Wall Temperature Comparison of Different H/D

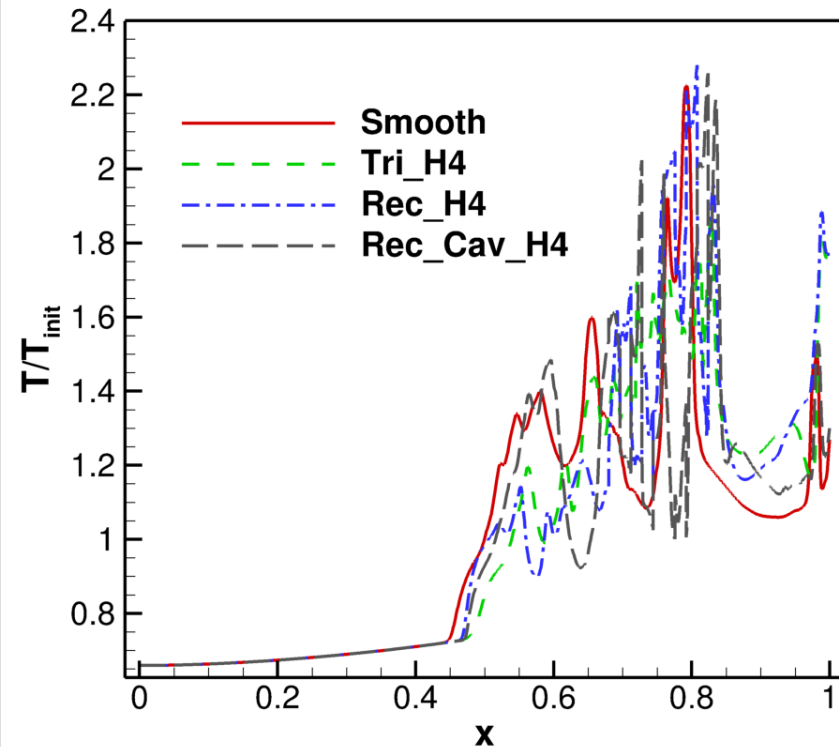


Overview of wall temperature

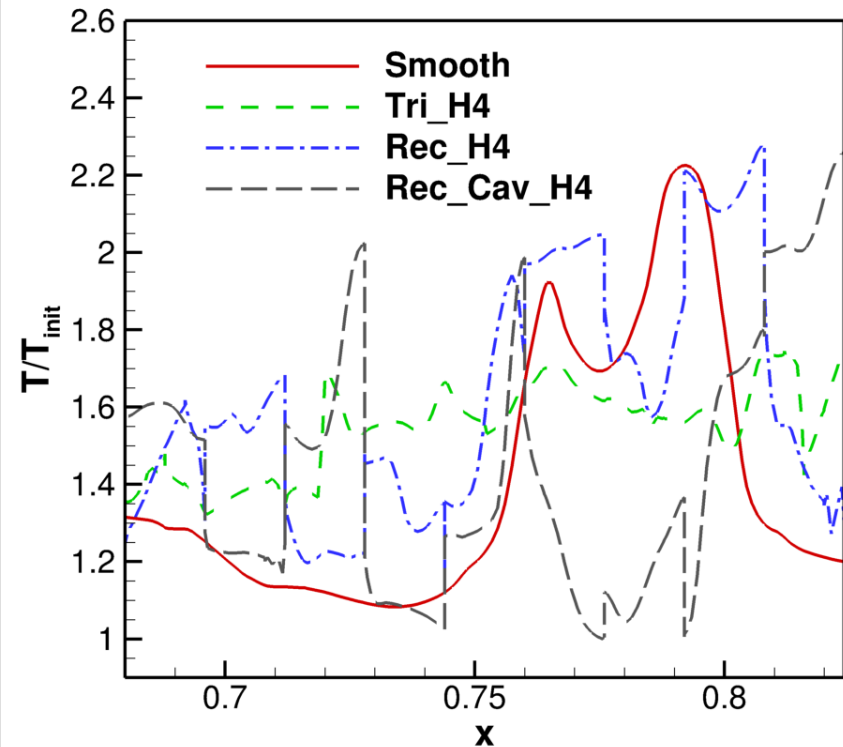


Close-up view of wall temperature

Wall Temperature Comparison of Different Types of Roughness Elements



Overview of wall temperature



Close-up view of wall temperature

Contents

- Background
- Numerical Methods & Verification
- Shock/Boundary Layer Interaction (SBLI)
 - SBLI over smooth walls
 - SBLI over surface roughness
- **Conclusions & Future Work**

Conclusions & Future Work

- ✚ A localized Laplacian artificial viscosity (LLAV) stabilization procedure is developed for the high-order unstructured-grid-based flux reconstruction/correction procedure via reconstruction (FR/CPR) method.
- ✚ The FR/CPR-LLAV method is used to simulate shock-boundary layer interaction (SBLI) with and without wall roughness.
 - The FR/CPR-LLAV method can sharply capture shock structures and efficiently resolve boundary-layer separation features
 - The FR/CPR-LLAV method is capable of flow simulation over complex geometry
 - The FR/CPR-LLAV method is compact, and therefore, is suitable for parallel computing

Conclusions & Future Work (Cont.)

- ✚ Effects of surface roughness on SBLI are numerically investigated.
 - Surface roughness can substantially modify the interaction between the shock and the boundary layer, thus affecting surface heat transfer processes
 - In the current 2D study, the triangular roughness elements with relatively large height-width ratio can enhance the mixing near the wall
 - The rectangular (cavity) roughness elements with relatively large height-width ratio can trap the evolving separation vortices, resulting in redistribution of surface temperature
- More studies on 2D roughness elements of different types
 - Extension to 3D shock-turbulence interaction

References

- **H. T. Huynh**, "A flux reconstruction approach to high-order schemes including discontinuous Galerkin methods," in the 18th AIAA Computational Fluid Dynamics Conference, Miami, FL, 2007.
- **Z. J. Wang** and **H. Y. Gao**, "A unifying lifting collocation penalty formulation including the discontinuous Galerkin, spectral volume/difference methods for conservation laws on mixed grids," Journal of Computational Physics, Vol. 228, pp. 8161-8186, 2009.
- **P. Vincent**, **P. Castonguay**, and **A. Jameson**, "A new class of high-order energy stable flux reconstruction schemes", Journal of Scientific Computing, Vol. 47, pp. 50-72, 2011.
- **M. L. Yu** and **Z. J. Wang**, "On the connection between the correction and weighting functions in the correction procedure via reconstruction method," Journal of Scientific Computing., vol. 54, no. 1, pp. 227-244, 2013.
- **M. L. Yu**, **Z. J. Wang** and **Y. Liu**, "On the accuracy and efficiency of discontinuous Galerkin, spectral difference and correction procedure via reconstruction methods," Journal of Computational Physics, Vol. 259, pp. 70-95, 2014.
- **P.-O. Persson** and **J. Peraire**, "Sub-cell shock capturing for discontinuous Galerkin methods," in the 44th AIAA Aerospace Sciences Meeting and Exhibit, Reno, NV, 2006.
- **M. L. Yu** and **Z. J. Wang**, "Shock capturing for the correction procedure via reconstruction method using artificial viscosity and diffusivity," in ICCFD8, Chengdu, China, 2014.
- **M. L. Yu**, **F. X. Giraldo**, **M. Peng** and **Z. J. Wang**, "Localized artificial viscosity stabilization of discontinuous Galerkin methods for nonhydrostatic mesoscale atmospheric modeling," report, Naval Postgraduate School.
- **B. Sjögren** and **H. C. Yee**, "Grid convergence of high order methods for multiscale complex unsteady viscous compressible flows," Journal of Computational Physics, Vol. 185, pp. 1-26, 2003.
- **V. Daru** and **C. Tenaud**, "Numerical simulation of the viscous shock tube problem by using a high resolution monotonicity-preserving scheme," Computers & Fluids, Vol. 38, pp. 664-676, 2009.

Thank you!